

EFFECTS OF ANNEALING ON THE PHYSICAL PROPERTIES OF ITO THIN FILMS GROWN BY RADIO FREQUENCY MAGNETRON SPUTTERING

A. RADU^a, C. LOCOVEI^{a,b}, V. A. ANTOHE^{a,c}, M. SOCOL^b, D. COMAN^a,
M. MANICA^a, A. DUMITRU^a, L. DAN^a, C. RADU^a, A. M. RADUTA^a, L. ION^a,
S. IFTIMIE^a, S. ANTOHE^{a,d,*}

^aUniversity of Bucharest, Faculty of Physics, 405 Atomistilor, Magurele, 077125, Ilfov, Romania

^bNational Institute of Materials Physics, 405A Atomistilor, Magurele, 077125, Ilfov, Romania

^cUniversité Catholique de Louvain (UC Louvain), Institute of Condensed Matter and Nanosciences (IMCN), Place Croix du Sud 1, B-1348 Louvain-la-Neuve, Belgium

^dAcademy of Romanian Scientists, Ilfov Street, No.3, 030167, Bucharest, Romania

Indium-doped tin oxide (ITO) thin films were fabricated by radio frequency magnetron sputtering and were subjected to *in-situ* and *ex-situ* annealing, at 200°C, 300°C and 400°C, respectively. The *in-situ* thermal treatment consisted to intentionally heating the samples' substrates, while the *ex-situ* annealing was performed using an oven, under ambient atmosphere. For the ITO samples subjected to *ex-situ* annealing, the density of oxygen vacancies increased leading to the decrease of the electrical resistivity. No significant changes were noticed in terms of transmission spectroscopy after the thermal treatment; while by evaluating the Skewness parameter was determined that the annealing improves the planarity of samples' surface.

(Received May 19, 2020; Accepted July 15, 2020)

Keywords: ITO, Magnetron sputtering, Annealing, Van der Pauw measurements

1. Introduction

Finding the appropriate transparent electrode for electronic and optoelectronic applications such as solar cells [1-4], light emitting diodes and organic emitting diodes [5-7], gas sensors [8,9], and liquid crystal displays [10] can be challenging for researchers due to a large number of requirements that should be accomplished in terms of physical and chemical properties. From various transparent conductive oxides based on metals, e.g. zinc oxide, aluminum-doped zinc oxide, gallium-doped zinc oxide, fluorine-doped tin oxide, etc., indium-doped tin oxide (ITO) is one of the most frequently used. Two important features recommend ITO, namely its high transparency, usually larger than 80%, [11] in the visible region of the electromagnetic spectrum and good conductivity at room temperature [12,13]. Moreover, the morphological, structural and electrical properties of ITO architectures are strongly sensitive to both growth method and post-deposition treatments [14-18]. ITO and ZnO versatility led to a variety of physical and chemical deposition methods, such as electron beam evaporation [19], pulsed laser ablation [20-22], spray-pyrolysis [23,24], electrochemical deposition [25-27], ion implantation [28], and magnetron sputtering [29]. In the case of 2D structures, radio frequency magnetron sputtering (RF-magnetron sputtering) growth method is popular and versatile because offers rigorous control of working parameters leading to high quality samples [30,31].

ITO is a highly degenerate n-type semiconductor for which tin atoms are replacing the indium ones [32,33], with partially formation of oxygen vacancies. Due to this particularity, thermal and chemical treatments [34,35] or electro-annealing [36] are becoming significant because its properties can be dramatically changed.

* Corresponding authors: santohe@solid.fizica.unibuc.ro

In this paper, we employ X-ray diffraction, atomic force microscopy, scanning electron microscopy, optical spectroscopy, and van der Pauw measurements to investigate the effects of annealing on the physical properties of ITO thin films fabricated by RF-magnetron sputtering. The results provide evidence that thermal treatments strongly influence the electrical and structural properties of obtained samples. Moreover, we demonstrated that such architectures are sensitive to annealing conditions.

2. Experimental procedures

ITO thin films were grown by RF-magnetron sputtering onto optical glass, under argon atmosphere, using a TECTRA setup containing three thin film deposition facilities (Thermal Vacuum Evaporation (TVE); Electronic Beam; and DC- and RF-magnetron sputtering) placed in a stainless steel deposition chamber. The sputtering target was commercially available from FHR Company, 99.99% purity, and was used without further purification. The distance between substrate holder and target was maintained constant during deposition, at 11 cm. Prior to the deposition process, the substrates were subsequently cleaned in acetone and distilled water for 15 min. 10 sets of samples were fabricated differing in the annealing, i.e. *in-situ* or *ex-situ*. The *in-situ* annealing consisted of the intentional heating of the substrates during deposition, at different temperatures (see Table1), while the *ex-situ* annealing was performed in air, using a Nabertherm oven with maximum reaching temperature of 1100°C. The heating rate was 1°C/min and the holding time was 10 minutes. The fabrication parameters of samples together with their evaluated thickness are summarized in Table1. The thickness of thin films was determined by X-ray reflectivity (XRR) using a Bruker D8 Discover diffractometer ($\text{Cu}_{\text{K}\alpha 1} = 1.5406 \text{ \AA}$). Same equipment was used to evaluate the structural features by grazing incidence X-ray diffraction (GIXRD), at an incidence angle of 0.7° . The morphological investigations were done by atomic force microscopy (AFM) using an A.P.E. Research equipment, in tapping mode, and by scanning electron microscopy using a Tescan Vega XMU-II machine, operating at 30 KV. Transmission spectroscopy spectra were acquired in the spectral domain of 300 nm – 1100 nm, in air, using a Perkin Elmer Lambda 750 spectrometer. The electrical behavior of fabricated ITO thin films was analyzed by van der Pauw measurements in the temperature ranges of 300 K – 10 K using a Janis cryogenic equipment with recirculation of helium, working up to a temperature of 4 K.

Table 1. Working parameters, the evaluated thickness and the type of annealing of fabricated ITO thin films by RF-magnetron sputtering.

Sample	Working pressure (Pa)	Working power (W)	Deposition time (min)	Temperature of annealing (°C)	Type of annealing	Thickness (nm)
Sample1	0.86	60	10	-	-	37
Sample2	0.86	80	10	-	-	47
Sample3	0.86	100	10	-	-	88
Sample4	0.86	100	10	100	<i>in-situ</i>	83
Sample5	0.86	100	10	200	<i>in-situ</i>	81
Sample6	0.86	100	10	300	<i>in-situ</i>	86
Sample7	0.86	100	10	400	<i>in-situ</i>	90
Sample8	0.86	100	10	200	<i>ex-situ</i>	81
Sample9	0.86	100	10	300	<i>ex-situ</i>	80
Sample10	0.86	100	10	400	<i>ex-situ</i>	83

3. Results and discussions

The GIXRD patterns of fabricated thin films are shown in Fig. 1. One can easily observe that when no annealing was made no crystalline arrangement was noticed. Basically, the samples 1, 2 and 3 are amorphous. By increasing the substrate temperature, the amorphous feature is not removed but an early crystallization can be detected. In the case of samples 8, 9 and 10 for which *ex-situ* annealing was performed at 200°C, 300°C and 400°C, respectively, the (222) and (400) peaks became clearly visible, indicating that the preferentially oriented textures are (111) and (100). The (222) maximum is associated with the bonded oxygen atoms located in the ITO thin films, while oxygen vacancies are preferential to occupy the (400) plane [32,36,37]. The increase of these two peaks after the *ex-situ* thermal treatment was an expected behavior; the increase of the density of oxygen vacancies has induced significant changes of the electrical behavior of fabricated samples. Also, other specific peaks of body-centered cubic structure can be identified, namely (440) and (622) as PDF file 00-006-0416 indicates.

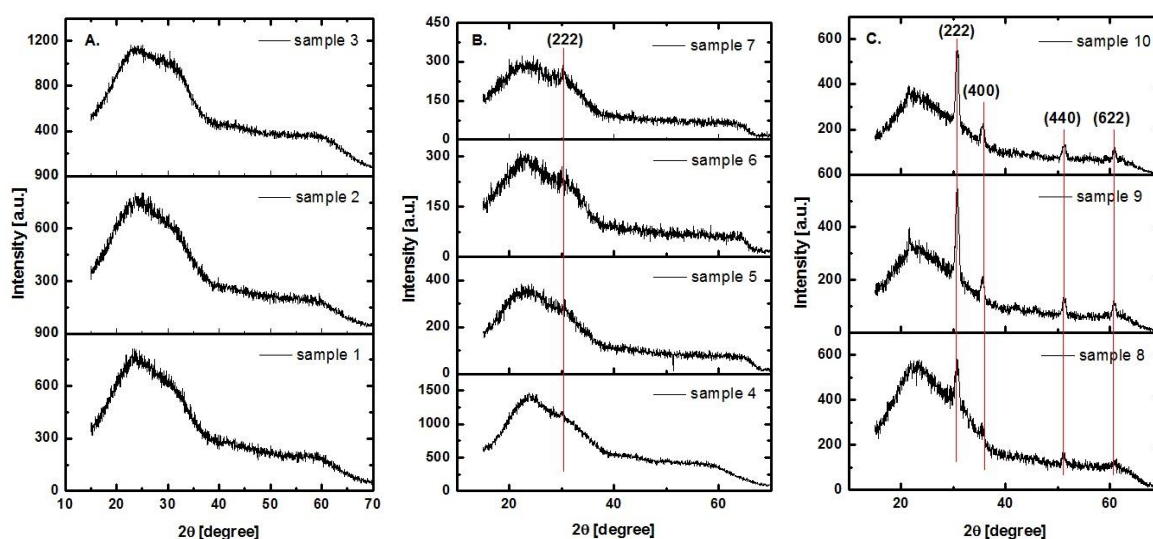


Fig. 1. GIXRD patterns of fabricated ITO thin films. (A) For samples 1, 2 and 3 no annealing was performed. (B) For samples 4, 5, 6, and 7, in-situ annealing was done by heating the substrate during the deposition process at 100°C, 200°C, 300°C, and 400°C, respectively. (C) For samples 8, 9 and 10, *ex-situ* annealing was done using a Nabertherm oven, in air, at 200°C, 300°C and 400°C, respectively.

The topography of the surface of prepared ITO samples was analyzed by AFM and SEM. In Fig. 2 are presented both the AFM images and the top-view SEM micrographs. Table 2 summarizes the calculated AFM parameters, e.g. root mean square (RMS), roughness average (R_a) and Skewness (Ssk).

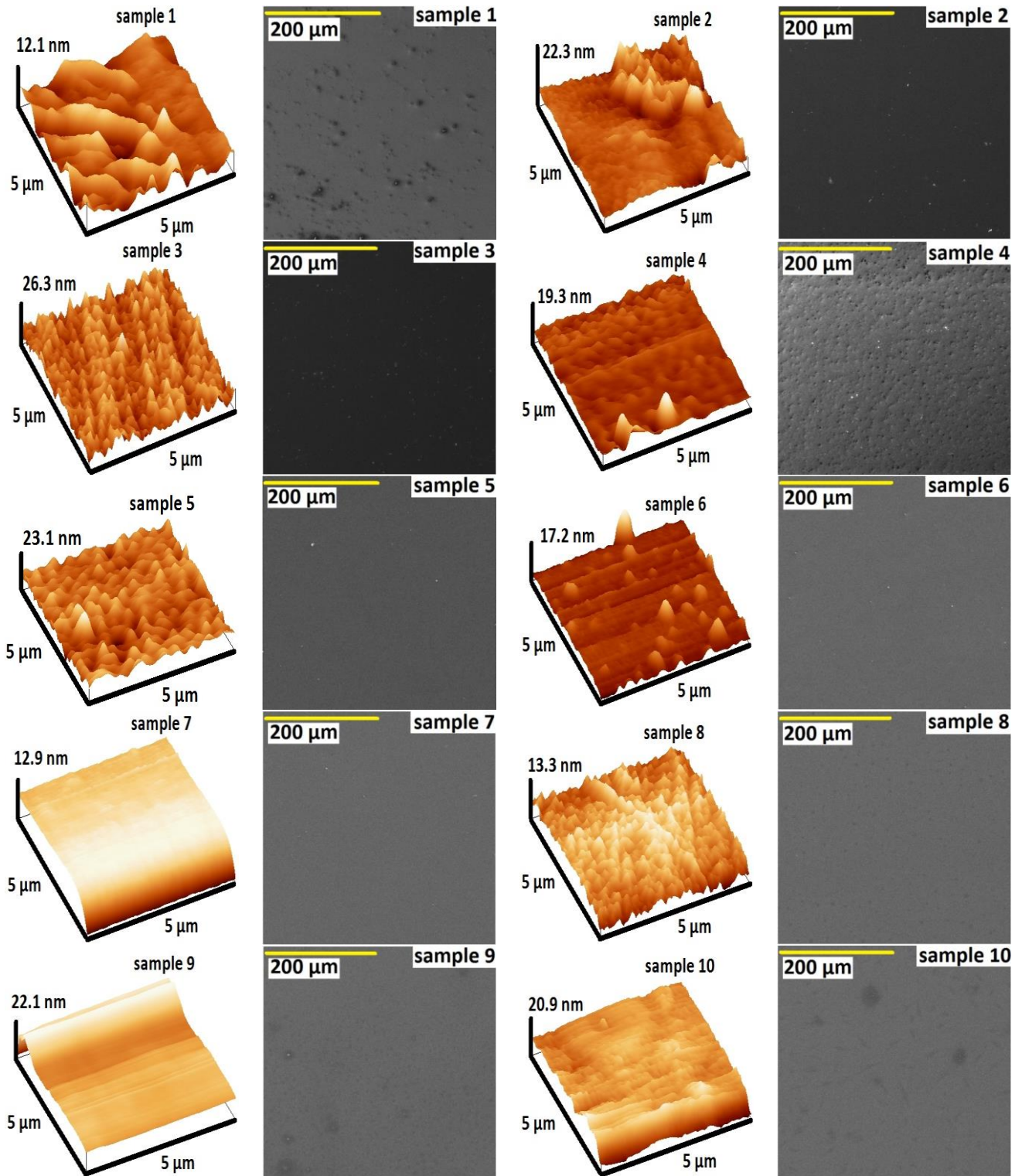


Fig. 2. 3D-topographic AFM images of the surface of prepared ITO thin films together with top-view SEM micrographs.

The surface of prepared ITO samples is mainly uniform and smooth, proving that magnetron sputtering is a suitable technique to grow thin films. Roughness average is calculated as the mean value of the surface height relatively to the center plane, while root mean square is the standard deviation of the surface height for an arbitrary area [38]. We expected that by increasing the annealing temperature, clusters to be form due to the aggregation of native grains as other

authors found [33,39] but this fact is not supported by either AFM parameters or SEM analyses of prepared layers, except for those samples annealed at 200°C, either *in-situ* or *ex-situ*. One may notice the slightly increase of RMS and R_a with the increase of working power in the case of those samples where no annealing was performed. This is mainly due to the increase of sticking coefficient with the increase of kinetic energy of ions that collide, so small grains aggregate leading to an increase of the roughness surface. Recently, similar results were reported by M. Shakiba and co-workers for ITO thin films deposited by DC-magnetron sputtering [32]. For the other grown thin films which *in-situ* or *ex-situ* thermal treatments were carried out, no correlation between temperature of annealing and RMS or R_a could have been made. An intriguing fact was observed for samples 8, 9 and 10 for which the Skewness parameter became more negatively with the increase of temperature of annealing. Skewness parameter describes the degree of asperity of thin films' surface. If the height distribution is skewed above the mean plane the calculated values are negative, indicating that valleys predominate over the peaks. The increase of Skewness in the negative part can be correlated with XRD results, and suggests an increase of planarity of the surface [40].

Table 2. Determined values of root mean square (RMS), roughness average (R_a) and Skewness (Ssk) for fabricated ITO thin films

Sample	Thickness (nm)	Root mean square (nm)	Roughness average (nm)	Skewness (nm)	Temperature of annealing (°C)	Type of annealing
Sample1	37	1.7	1.3	0.4	-	-
Sample2	47	2.5	2.0	0.7	-	-
Sample3	88	3.1	2.5	0.2	-	-
Sample4	83	4.3	4.2	2.5	100	in-situ
Sample5	81	4.7	4.6	0.2	200	in-situ
Sample6	86	1.6	2.4	1.9	300	in-situ
Sample7	90	1.8	1.8	-2.2	400	in-situ
Sample8	81	3.8	3.4	-0.1	200	ex-situ
Sample9	80	1.8	2.0	-0.9	300	ex-situ
Sample10	83	3.3	2.3	-1.2	400	ex-situ

The transmission spectroscopy spectra of fabricated ITO thin films together with the results for glass substrates are shown in Figure3. For all samples, the average transparency is larger than 75% in the visible domain. A slight increase of optical transmission can be identified for samples 8, 9 and 10, compared with the others. Due to the increase of structural order the extinction coefficient decreases because the point-like defects are partially removed by annealing, so the absorption coefficient decreases too [41].

The electrical behavior of prepared ITO structures was analyzed by van der Pauw measurements from room temperature (RT) to 10 K (see Figure4). The electrical resistivity was determined from a total of 8 measurements that were made around the periphery of thin films, using the following expressions:

$$\rho_1 = \frac{\pi}{\ln 2} \times f_1 \times d \times \frac{(V_1 - V_2 + V_3 - V_4)}{4I}$$

$$\rho_2 = \frac{\pi}{\ln 2} \times f_2 \times d \times \frac{(V_5 - V_6 + V_7 - V_8)}{4I}$$

in which ρ_1 and ρ_2 are volume resistivity, expressed in $\Omega \times m$, d is the thickness of fabricated ITO thin films, $V_1 - V_8$ are the experimentally determined electrical voltages, I is the electrical intensity, and f_1 and f_2 are geometrical factors. Assuming samples have perfect symmetry, f_1 and f_2 were considered equals with unit.

After ρ_1 and ρ_2 were known, the average electrical resistivity was determined as arithmetic mean of them.

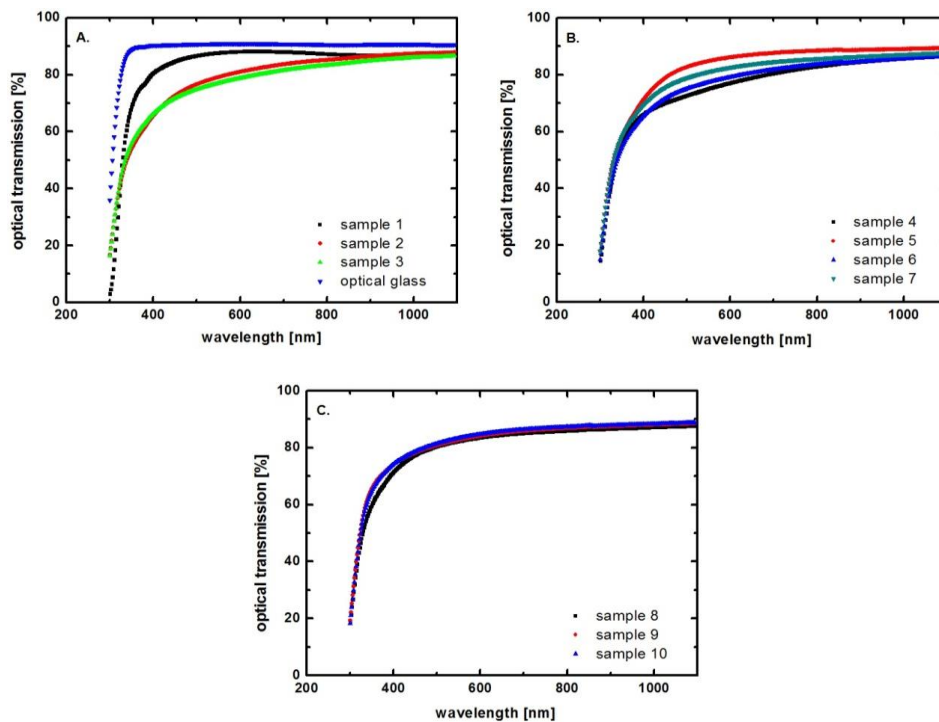


Fig. 3. Optical transmission spectra of fabricated ITO thin films. For the purposes of comparison the obtained results of glass substrates are given (figure3A – blue curve).

One can easily notice that there is a significant difference between as prepared samples and those who were thermally treated *ex-situ*, i.e. the electrical conductivity increases with the increase of annealing temperature. This behavior should be explained in the frame of GIXRD results that have indicated the increase of the density of oxygen vacancies. We expected this, taking into account that the annealing was done in ambient atmosphere. Ideally, each oxygen vacancy can transfer 2 electrons in the conduction band so the density of free charge carriers is significantly increased [32].

An interesting result was registered in the case of sample 4, for which the electrical conductivity values are really good, similar with those determined for sample 9 for which the annealing temperature was 300°C, *ex-situ*. For sample 4 the annealing temperature was 100°C, *in-situ*. Our assumption is that the tin (Sn) atoms from indium oxide lattice were activated and this led to an overall increase of the electrical conductivity.

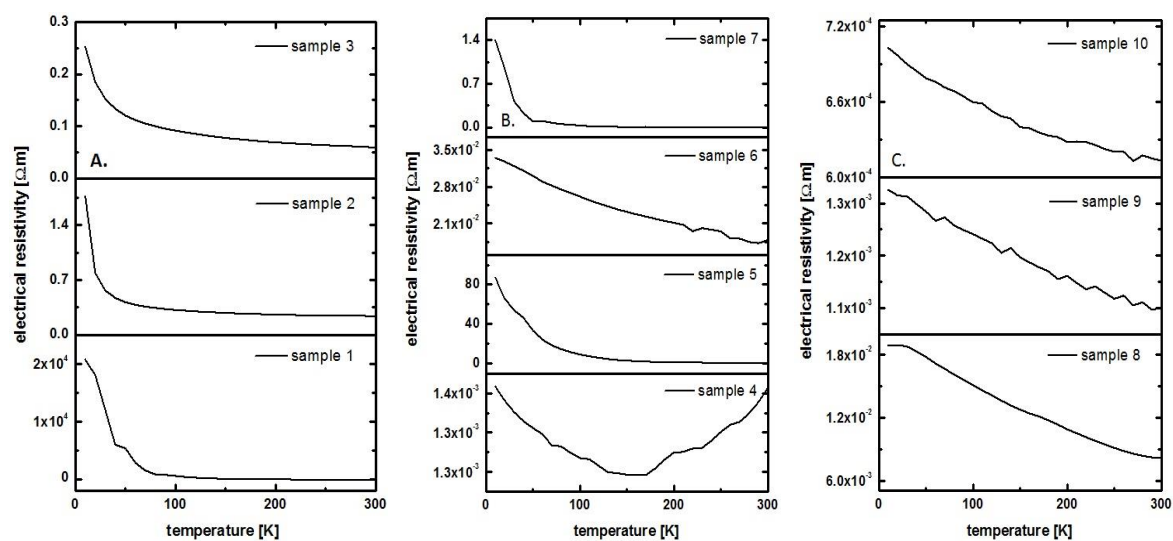


Fig. 4. Electrical resistivity of fabricated ITO thin films determined by van der Pauw measurements in the temperature range of RT – 10 K.

4. Conclusions

Effects of annealing, i.e. *in-situ* and *ex-situ*, on the physical properties of ITO thin films grown by RF-magnetron sputtering were investigated. The *in-situ* thermal treatment was performed by heating the sample substrates during the deposition process, while the *ex-situ* annealing was done using an oven, under ambient atmosphere. The annealing temperatures were 200°C, 300°C and 400°C, respectively. As expected, the number of oxygen vacancies was increased for ITO thin films subjected to *ex-situ* annealing. Also, for all treated samples was observed the increase of number of bonded oxygen atoms with the increase of annealing temperature. Notwithstanding, no significant changes were noticed for pristine samples and thermally treated ones in terms of optical transmission. In the case of ITO samples subjected to *ex-situ* annealing, by evaluating the Skewness parameter from AFM measurements was observed that the planarity of the surface improves with the rise of temperature. Because the number of oxygen vacancies was increased, the electrical conductivity was significantly increased, even with 5 orders of magnitude. We demonstrated that the *ex-situ* annealing led to better crystallinity, planarity of the surface and electrical conductivity in terms of pristine and *in-situ* treated samples.

Acknowledgements

Support from Executive Unit for Financing Higher Education, Research, Development and Innovation (UEFISCDI) through grant no. 18PCCDI/2018, no. 11844/2012 and grant no. 40PCCDI/2018 is acknowledged.

References

- [1] C. Sima, C. Grigoriu, S. Antohe, Thin Solid Films **519**(2), 595, (2010)
- [2] M. Radu, V. Ghenescu, I. Stan, L. Ion, C. Besleaga, A. Nicolaev, T. L. Mitran, C. Tazlaoanu, A. Radu, O. Porumb, M. Ghenescu, M. Gugiu, S. Antohe, Chalcogenide Letters **8**(8), 477 (2011).
- [3] S. Iftimie, C. Tazlaoanu, A. Radu, R. Constantineanu, C. Vancea, N. Korganci, L. Ion, S. Antohe, Digest Journal of Nanomaterials and Biostructures **9**(1), 213 (2014).
- [4] S. Antohe, S. Iftimie, L. Hrostea, V. A. Antohe, M. Girtan, Thin Solid Films **642**, 219 (2017).

- [5] Y. H. Tak, K. B. Kim, H. G. Park, K. H. Lee, J. R. Lee, *Thin Solid Films* **411**(1), 12 (2002).
- [6] D. Vaufrey, M. Ben Khalifa, J. Tardy, C. Ghica, M. G. Blanchin, C. Sandu, J. A. Roger, *Semiconductor Science and Technology* **18**(4), 253 (2003).
- [7] A. B. Djuricic, C. Y. Kwong, P. C. Chui, W. K. Chan, *Journal of Applied Physics* **93**(9), 5472 (2003).
- [8] E. Comini, G. Faglia, G. Sberveglieri, *Sensors and Actuators B: Chemical* **78**(1-3), 73 (2001).
- [9] Z. Tang, P. C. H. Chan, R. K. Sharma, G. Yan, I. M. Hsing, J. K. O. Sin, *Sensors and Actuators B: Chemical* **79**(1), 39 (2001).
- [10] S.-C. Hsu, D.-S. Wu, X. Zheng, R.-H. Horng, *Journal of the Electrochemical Society* **156**(4), H281 (2009).
- [11] C. Besleaga, L. Ion, G. Socol, A. Radu, I. Arghir, C. Florica, S. Antohe, *Thin Solid Films*, **520**(22), 6803 (2012)
- [12] G. Socol, D. Craciun, I. N. Mihailescu, N. Stefan, C. Besleaga, L. Ion, S. Antohe, K. W. Kim, D. Norton, S. J. Pearton, A. C. Galca, V. Craciun, *Thin Solid Films* **520**(4), 1274 (2011).
- [13] W. F. Wu, B. S. Chiou, *Semiconductor Science and Technology* **11**(2), 196 (1996).
- [14] O. Tuna, Y. Selamet, G. Aygun, L. Ozyuzer, *Journal of Physics D: Applied Physics* **43**(5), 055402 (2010).
- [15] A. Rogozin, N. Shevchenko, M. Vinnichenko, M. Seidel, A. Kolitsch, W. Moller, *Applied Physics Letters* **89**(6), 061908 (2006).
- [16] Y. Pei, L. Lin, W. Zheng, Y. Qu, Z. Huang, F. Lai, *Surface Review and Letters* **16**(06), 887 (2009).
- [17] D. Lee, S. Shim, J. Choi, K. Yoon, *Applied Surface Science* **254**(15), 4650 (2008).
- [18] C. Palade, A. Slav, A. M. Lepadatu, I. Stavarache, I. Dascalescu, A. V. Maraloiu, C. Negrila, C. Logofatu, T. Stoica, V. S. Teodorescu, M. L. Ciurea, S. Lazanu, *Nanotechnology* **30**(44), 445501 (2019).
- [19] H. M. Ali, H. A. Mohamed, S. H. Mohamed, *The European Physical Journal Applied Physics* **31**(2), 87 (2005).
- [20] F. O. Adurodija, H. Izumi, T. Ishihara, H. Yoshioka, K. Yamada, H. Matsui, M. Motoyama, *Thin Solid Films* **350**(1-2), 79 (1999).
- [21] M. Socol, N. Preda, C. Breazu, A. Stanculescu, A. Costas, F. Stanculescu, M. Girtan, F. Gherendi, G. Popescu-Pelin, G. Socol, *Applied Physics A: Materials Science & Processing* **124**(9), 602 (2018).
- [22] M. Socol, N. Preda, O. Rasoga, A. Costas, A. Stanculescu, C. Breazu, F. Gherendi, G. Socol, *Coatings* **9**(1), 19 (2019).
- [23] S.M. Rozati, T. Ganj, *Renewable Energy* **29**(10), 1671 (2004).
- [24] I. Vaiciulis, M. Girtan, A. Stanculescu, L. Leontie, F. Habelhames, S. Antohe, *Proceedings of the Romanian Academy Series A-Mathematics Physics Technical Sciences Information Science* **13**(4), 335 (2012)
- [25] V. A. Antohe, L. SK Srivastava, L. Piraux, *Nanotechnology* **23** (25), 255602 (2012).
- [26] V. A. Antohe, M. Mickan, F. Henry, R. Delamare, L. Gence, L. Piraux, *Applied Surface Science* **313** 607 (2014)
- [27] D. Tamvakos, S. Lepadatu, V. A. Antohe, A. Tamvakos, P. M. Weaver, L. Piraux, M. G. Cain, D. Pullini, *Applied Surface Science* **356**, 1214 (2015).
- [28] M. Sawada, M. Higuchi, *Thin Solid Films* **317**(1-2), 157 (1998).
- [29] G. Giusti, L. Tian, I. P. Jones, J. S. Abell, J. Bowen, *Thin Solid Films* **518**(4), 1140 (2009).
- [30] C. Besleaga, G. E. Stan, A. C. Galca, L. Ion, S. Antohe, *Applied Surface Science* **258**(22), 8819 (2012).
- [31] C. Sima, C. Grigoriu, O. Toma, S. Antohe, *Thin Solid Films* **597**, 206 (2015)
- [32] M. Shakiba, A. Kosarian, E. Farshidi, *Journal of Materials Science: Materials in Electronics* **28**(1), 787 (2017).
- [33] D. Raoufi, A. Kiasatpour, H. R. Fallah, A. S. H. Rozatian, *Applied Surface Science* **253**(23), 9085 (2007).
- [34] M. Duta, M. Anastasescu, J. M. Calderon-Moreno, L. Predoana, S. Preda, M. Nicolescu, H. Stroescu, V. Bratan, I. Dascalu, E. Aperathitis, M. Modreanu, M. Zaharescu, M. Gartner, *Journal of Materials Science: Materials in Electronics* **27**(5), 4913 (2016).

- [35] S. Luo, K. Okada, S. Kohiki, F. Tsutsui, H. Shimooka, F. Shoji, *Materials Letters* **63**(6-7), 641 (2009).
- [36] H. Koseoglu, F. Turkoglu, M. Kurt, M. D. Yaman, F. G. Akca, G. Aygun, L. Ozyuzer, *Vacuum* **120**, 8 (2015).
- [37] S. I. Jun, T. E. McKnight, M. L. Simpson, P. D. Rack, *Thin Solid Films* **476**(1), 59 (2005).
- [38] C. Locovei, D. Coman, A. Radu, L. Ion, V. A. Antohe, N. Vasile, A. Dumitru, S. Iftimie, S. Antohe, *Thin Solid Films* **685**, 379 (2019).
- [39] F. Matino, L. Persano, V. Arima, D. Pisignano, R. I. R. Blyth, R. Cingolani, R. Rinaldi, *Physical Review B* **72**(8), 085437 (2005).
- [40] H. H. Yudar, S. Korkmaz, S. Ozen, V. Senay, S. Pat, *Applied Physics A: Materials Science & Processing* **122**(8), 748 (2016).
- [41] V. Gupta, A. Mansingh, *Journal of Applied Physics* **80**(2), 1063 (1996).